JOURNAL OF PROPULSION AND POWER
Vol. 24, No. 5, September–October 2008

Characterization of a Prefilming Airblast Atomizer in a Strong Swirl Flowfield

R. Kumara Gurubaran,* R. I. Sujith,† and S. R. Chakravarthy‡
Indian Institute of Technology, Madras, Chennai 600 036, India

DOI: 10.2514/1.35012

Most gas turbine engines in service use a prefilming airblast atomizer in combination with strong swirling flow. An experimental investigation of the characteristics of a hollow cone prefilming airblast atomizer in a strong swirling air flow is presented in this paper. The measured quantities include the spray cone angle by planar imaging, patternation using planar laser-induced fluorescence, planar droplet velocity field using two-component particle image velocimetry, and droplet size and velocity distributions using a phase Doppler particle-size analyzer and laser Doppler velocimetry. Patternation of the spray field showed regions of high droplet concentration and volume flux fluctuations in various cross-sectional planes. The investigation revealed the presence of droplets of narrow size range up to 25 μ around the axis of the atomizer in the central toroidal recirculation zone of the swirler. The presence of vortical structures entraining the droplets is observed from the instantaneous velocity vector fields. The velocity data shows entrainment of the droplets in the central toroidal recirculation zone. Examining the size and the velocity data reveals that the centrifugal action of the swirling air flowfield from the atomizer carries the bigger droplets outward, toward the periphery of the spray.

I. Introduction

LIQUID fuels are injected into combustion chambers by means of atomizers. Fuel injection plays a major role in many aspects of combustor performance, such as stability limits, combustion efficiency, and pollutant emission levels. Therefore, it is important to know the details of the fuel injector performance. The structure of fuel sprays in gas turbine combustors is complex and varies both temporally and spatially. Slight imperfections in the fuel nozzle lip can yield significant variations in fuel spray pattern [1]. Nonuniform spray patterns can result in poor mixing between fuel and air, which lowers the combustion efficiency and increases emitted pollutants. The actual conditions of spray injection, dispersion, vaporization, and burning of the fuel with different stoichiometric proportions of air in a well-mixed environment affect the combustion stability, efficiency, and pollutant formation. Specifically, fuel–air mixing and the time–temperature dwell history of the fuel droplets determine the quality of combustion and the levels of emissions generated.

There are many types of atomizers used in gas turbine engines. Most gas turbine engines in service use prefilming type of airblast atomizers because of their potential for achieving significant reductions in soot formation and exhaust smoke. The prefilming concept for airblast atomization evolved from the studies of Lefebvre and Miller [2]. Rizkalla and Lefebvre [3] investigated the effects of both air and liquid properties on atomization quality. They reported that for liquids of low viscosity, the mean drop sizes obtained are inversely proportional to air velocity and air density and are directly proportional to the square root of both liquid density and liquid surface tension. Atomization quality deteriorates with increase in liquid viscosity and liquid–air mass ratio. Rizk and Lefebvre [4] studied the influence of air velocity and liquid properties on the drop size distribution in an airblast atomizer. They concluded that high values of liquid viscosity and liquid flow rate resulted in thicker liquid films, leading to coarser sprays. The increase in annulus height, air velocity, and air density gave thinner films and, hence, better atomization. Han et al. [1] investigated the effects of the fuel nozzle displacement on the spray characteristics. They found that there was significant variation in cone angle, droplet number density, and recirculation pattern of the spray.

To obtain flame stabilization in a combustor, a region of flowfield must be found where the flame speed matches the forward flow velocity, and, also, the heat supplied must be sufficient to initiate the combustion process. This is accomplished by imparting a swirl to the flowfield. Flows with a high degree of swirl are characterized by the presence of a central toroidal recirculation zone (CTRZ), high turbulence, and combustion intensity, which aid in flame stabilization and better performance of the combustor [5]. Brena de la Rosa et al. [6] conducted studies on the velocity and turbulence field of a solid cone spray from a pressure atomizer in swirling flowfields with low, medium, and high swirl numbers. From the spatial distribution of droplets, they showed that the spray widens with increasing swirl strength. The concentration of large drops increases near the core of the swirling field with increasing swirl number. Further, they showed that, due to flow reversal, droplets with sizes of the order of 5–10 μ recirculate in the core recirculation region at high swirl numbers.

Swirl flows have a large-scale effect on flowfields. For example, in the case of inert jets, swirl affects the jet growth, entrainment and decay, and, for reacting flows, the flame size, shape, stability, and combustion intensity. Reddy et al. [7] reported a decay of the tangential velocity along the flow path. The swirl motion decreased, and the flow transitioned to an axial flow with vanishing radial and tangential velocities, and the turbulence intensity decays toward downstream of the flow from the swirler.

Although considerable work has been done to study the phenomenon involved in swirl flows and sprays from prefilming airblast atomizers, not much information is available on the effect of swirl flow on the spray field, particularly for the case of hollow cone sprays. A hollow cone prefilming airblast atomizer in a strong swirl air flowfield with swirl number of 1.09 is used for the present study, which was conducted under atmospheric conditions. Planar laser-induced fluorescence (PLIF) was used to examine the liquid fuel distribution pattern (patternation) of the spray. Particle image velocimetry (PIV) was used to study the planar velocity distribution

Presented as Paper 4148 at the 41st AIAA/ASME/SAE/ASEE Joint Propulsion Conference and Exhibit, Tucson, AZ, 10–13 July 2005; received 6 October 2007; revision received 12 April 2008; accepted for publication 18 April 2008.

*Graduate Student, Department of Aerospace Engineering.
†Professor, Department of Aerospace Engineering. Member AIAA
‡Associate Professor, Department of Aerospace Engineering. Member AIAA

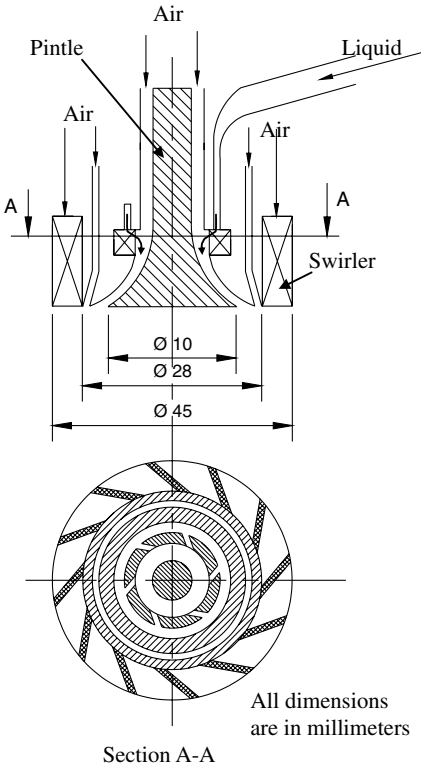

Fig. 1 Schematic of the prefilming airblast atomizer with swirler.

of the spray in various air–liquid ratios (ALRs). Three-component laser Doppler velocimetry and phase Doppler particle-size analyzer (3C-LDV/PDPA) were used to measure the three components of velocity and sizes, respectively, of the droplets in the spray field for various air–liquid ratios under atmospheric conditions.

II. Experimental Details

A. Experimental Setup

The experimental setup employed in the present study consists of a pressurized liquid fuel supply system, an air supply system, an injector assembly, and a liquid collection system. Air from the compressor passes through a regulator, a control valve, and a flow meter and enters the frontal device adapter. The air pressure is measured at this adapter.

The schematic of the prefilming airblast atomizer with the swirler is shown in Fig. 1. The swirler assembly has 12 helical vanes in it and is mounted around the injector in the frontal adapter. The swirler has an inner (hub) diameter of 33 mm and an outer diameter of 40 mm, and contains 12 straight vanes at an angle of 50 deg to the freestream direction. A photograph of the swirler is given in [7]. The effective area of air passage through the swirler is 215.9 mm^2. The fuel nozzle employed in this study is a prefilming airblast atomizer. The effective air flow area through the atomizer is 94.6 mm^2. Water is used as a surrogate fuel in the study. The maximum liquid flow rate is 0.51 l/ min for the atomizer. Steady liquid injection is obtained from the tank pressurized by nitrogen. The estimated uncertainty for volume flow measurements of liquid and air using rotameters is 2% of the full-scale range. The estimated uncertainty in ALR measurements is 4.5%.

B. Cone Angle Studies

A pulsed frequency-doubled neodymium-doped yttrium-aluminum-garnet laser (Nd-YAG, Big Sky Laser model manufactured by Quantel, France, wavelength 532 nm) was used as a source of illumination for the cone angle measurements. Using a combination of spherical and cylindrical lenses, the circular beam from the laser was converted to a sheet, approximately 1 mm thick. A charge-coupled device (CCD) camera (PixelFly model, PCO Imaging, Inc., Germany) having a resolution of 1360×1024 is used to image the flowfield. Experiments were performed for the seven air–liquid ratios shown in Table 1. More than 500 instantaneous images were acquired and ensemble averaged to measure the cone angle of the spray field. The lips of the atomizer prefilming surface were fixed as starting point, and the lines were drawn parallel to the outer hollow cone spray boundary from the lip of the atomizer exit to 30 mm downstream of the atomizer exit to measure the cone angle. The cone angle reported is the full cone angle. This takes care of the asymmetry in the flow. The uncertainty in the cone angle measurements is estimated to be 1 deg.

C. Planar Laser-Induced Fluorescence

The PLIF signal from a droplet is directly proportional to the volume of the droplet [8,9] in the absence of absorption. Hence, the PLIF signal intensity integrated over a cross section is proportional to the local liquid volume fraction of the fluid. Fluorescence intensity $i = ad^n$, where a is a constant and n is the exponent of the dependence of droplet diameter that depends on the dye concentration present in the liquid. The key factor in most applications of planar laser-induced fluorescence is the choice of the fluorescent tracer to mark the liquid. In the present work, water is mixed with 0.01 g/l Rhodamine 6G, which is well suited for PLIF experiments at a wavelength of 532 nm [10]. The images acquired at different cross sections are normalized, keeping in mind that the same volume of fluid passes through all the cross sections. In this experiment, the second harmonic of an Nd:YAG laser at 532 nm with up to 30 mJ per pulse of approximately 8 ns width is used.

Volume fraction measurements were performed from 15 to 50 mm down stream of the atomizer at 5 mm intervals to study the spread of the spray and its patternation. Five hundred instantaneous images were averaged to obtain the ensemble image of the spray. High concentration with clustering of the liquid phase are observed in the planar Mie scattering images up to 10 mm downstream form the exit of the atomizer. Therefore, PLIF images at 15 mm downstream from the exit of atomizer were used for normalization in patternation of spray field from the atomizer. The ensemble-averaged image at different downstream location is normalized with the ensemble-averaged image at 15 mm downstream location from the atomizer. This normalization essentially removes the spatial variation of the illumination intensity. Both the images have the same spatial variation, and it gets divided out giving a normalized image which is flat field corrected.

The dimension of the laser sheet (approximately Gaussian at its waist) at the field of interest (100×100 mm^2) is 150 mm $\times$ 1.5 mm.

Table 1 Experimental flow conditions

Air–liquid ratio	Air flow rate, l pm	Liquid flow rate, ccm	Reynolds no., Re	Air inlet velocity, m/s	Pressure drop Δp, bar
5.43	1250	270	344,417	10.4	0.028
8.48	1550	210	427,077	12.9	0.042
8.05	1600	230	440,854	13.3	0.045
7.00	1675	280	461,519	13.9	0.049
5.93	1775	350	48,907	14.8	0.057
5.14	1850	420	509,738	15.4	0.062
4.42	1925	510	530,403	16.0	0.068

The laser sheet intensity is fairly uniform in the region of investigation. The sheet optics, laser sheet intensity, and camera parameters were maintained constant. The distance between the atomizer exit and laser sheet is varied by moving the frontal adaptor, which houses the atomizer. The uncertainty in the patternation of the spray for measurements of the volume flux is caused by the uncertainty in PLIF signal intensity and image processing. The uncertainty in volume fraction is estimated as 1.2%.

D. Particle Image Velocimetry

PIV is a whole-field planar velocity measurement technique. A twin resonator, frequency-doubled, Nd:YAG laser designed for PIV measurements having 30 mJ energy per pulse was used as the source of illumination. Using a combination of spherical and cylindrical lenses, the circular beam from the laser was converted to a sheet approximately 1 mm thick. Special care was taken to ensure that the double-pulsed laser sheets overlap completely with each other at the measurement section, satisfying a requirement for successful PIV imaging. Two images separated by a short interval (of the order of 3 μs) were acquired using a full frame interline transfer CCD camera with a spatial resolution of 1024×1280 pixels, and gray scale resolution of 12 bits (Sensicam, from PCO imaging).

The present investigation was performed for the air–liquid ratios shown in Table 1. The height of the investigated region is about 75 mm downstream from exit of nozzle for velocity measurements. It is not possible to perform any velocity measurements up to 10 mm downstream of the nozzle, because the liquid is in the form of ligaments, the spray is too dense, and large droplets are present in that region. PIV images were analyzed using the cross-correlation software PivView 2C [11].[§] The interrogation size was 64×64 pixels with a 75% overlap between interrogation windows. Up to 252 samples were used to determine the mean velocities of the examined flowfield.

The displacement resolution was 5% of the mean displacement, based on a subpixel resolution of 0.2 pixels [12]. In traditional PIV, in which airflows are seeded with small droplets of 1 μm diameter, the interrogation window is chosen such that there are no significant velocity gradients within the window. However, it must be noted that a spray has particles that respond differently to the velocity fluctuations depending on their Stokes number $\sqrt{\nu/\omega d^2}$, where ν is the kinematic viscosity, ω is the angular frequency of the fluctuations, and d is the particle diameter. Hence, PIV gives an "estimate" of the average velocity [13]. A comparison of the velocity measurement from PIV was compared with LDV measurements, and they were found in good agreement [14].

E. Laser Doppler Velocimetry and Phase Doppler Particle-Size Analyzer

The point measurements of droplet size and three-dimensional velocities were acquired using a three-dimensional PDPA system (TSI, United States of America). The laser used for the present experimental study is an argon ion laser (Coherent Innova 70C, U.S. make). The multicolor laser beam is split and separated into three pairs of colors, that is, green (514.5 nm), blue (488 nm), and violet (476.5 nm). One part of each pair of the beam is shifted in optical frequency by 40 MHz from the other by means of a Bragg cell. The green and blue pairs of beams go to one fiber optic transceiver probe and the violet beam to another fiber optic transceiver. The fiber optic transceivers are mounted on a three-axis traverse system whose movement is controlled remotely from a computer. The green pair of beams is aligned along the main flow direction and at 40 deg with respect to the receiver optics. The violet pair of the beams is positioned at 30 deg with respect to the receiver optics. The angle between the two transceivers is 70 deg. The velocities of the droplets are transformed into orthogonal coordinates, details of which are given in [14]. The width of the probe volume has a maximum size of 155 μm, depending on the optical arrangement of the transceiver optics. The dominant mode is refraction for the selected optical arrangement.

The individual droplet sizes and their three-component velocities are acquired at each location in the spray field for every experimental condition. Data was acquired along five cross-sectional planes: 12, 20, 30, 40, and 50 mm downstream of the atomizer exit. In each cross-sectional plane, data was acquired at points 5 mm apart, from −50 to 50 mm along the radial locations.

The worst case uncertainty in the velocity measurements with the measured mean velocity is 1.2% [15]. Uncertainty of the PDPA based on phase angle resolution is 1 μm.

III. Results and Discussion

In the present study, an experimental investigation was performed on a spray from a prefilming airblast atomizer in a swirl flowfield under atmospheric exit conditions. The swirl number of the vane swirler used in the present study is 1.09, which corresponds to strong swirl [5]. Although experiments were performed for the air–liquid ratios shown in Table. 1, data for only select conditions is presented in this paper to highlight the most important physical aspects of the spray field. The results for all the test conditions in Table 1 are presented in [14].

A. Cone Angle Studies

The instantaneous images acquired for the cone angle measurement from the prefilming airblast atomizer flowfield are shown in Fig. 2. The ensemble average of 500 of these instantaneous images and the cone angle measurements are shown in Fig. 3 for two ALRs. As seen from the trend in Fig. 4, the cone angle increases with increase in the pressure drop across the atomizer. Apart from the cone angle measurements, the instantaneous images (not acquired at high frame rates, but at random instants) reveal that the liquid film separation from the atomizing lip is neither continuous nor uniform. The breakup of the liquid sheet from the atomizer lip is highly unsteady (see Fig. 2). Because of this unsteadiness in ligament breakup, clusters of droplets are observed in the atomizer flowfield.

B. Patternation Studies

The symmetry of the spray pattern produced by atomizers is an important variable in most practical applications. In gas turbine combustors, the fuel must be distributed uniformly to achieve high combustion efficiency, low pollutant emissions, and long life of turbine blade.

The ensemble average of 500 PLIF images is obtained at various cross-sectional planes of the spray flowfield. The ensemble-averaged images acquired at different cross-sectional planes normalized with the ensemble-averaged image 15 mm downstream from the prefilming airblast atomizer exit shows the dispersion and spread of the liquid droplets in each cross-sectional plane. The contour plots

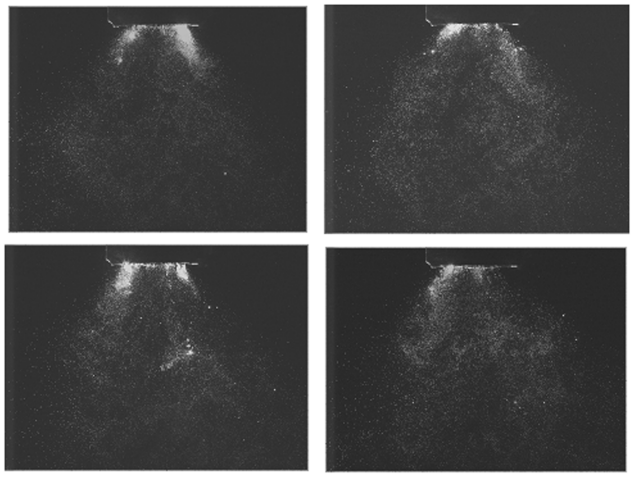

Fig. 2 Instantaneous Mie scattering images at an ALR of 7.00.

[§]Information available online at http://www.pivtec.com [retrieved 20 January 2007].

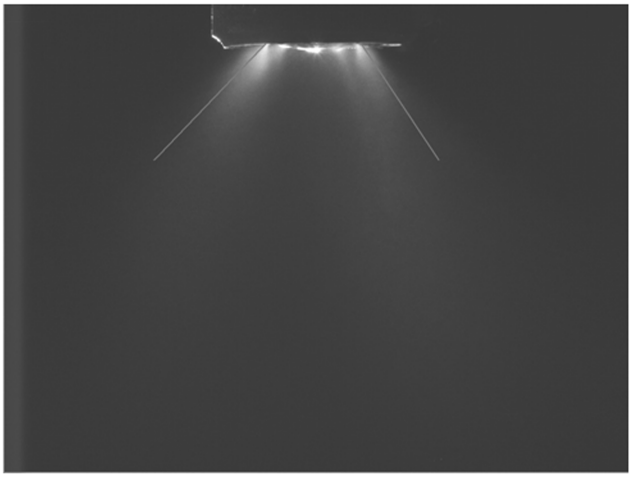

a)

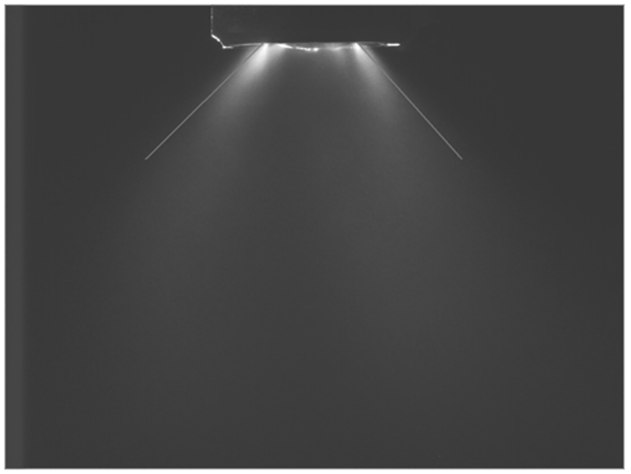

b)

Fig. 3 Cone angle measurement: ensemble-averaged image at an a) ALR of 5.43 and b) ALR of 7.00.

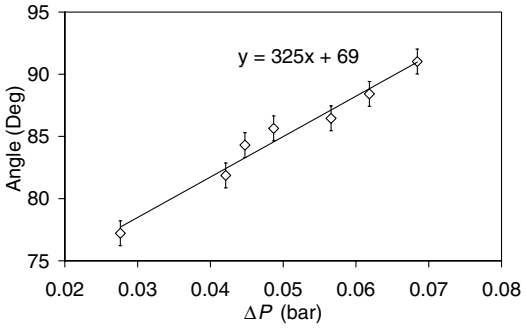

Fig. 4 Spray cone angle as a function of air pressure drop across the atomizer.

reveal the mixing and spread of the liquid mass flow with that of the air mass flow from the atomizer. A high concentration region is noticed at the cross-sectional plane 15 mm downstream from the atomizer exit for all ALRs considered in this study. Figure 5 shows the patternation contours for the ALR of 5.43. At this condition, the patternation images show that the droplets tend to be more or less spread and mixed 30 mm downstream from the atomizer. The regions of high droplet density can be noticed in the images at 15, 20, and 25 mm downstream of the atomizer exit. The high density region is due to the six liquid guide vanes in the atomizer liquid injector. The region of high droplet density is noticed up to 40 mm downstream of the atomizer in the case of an ALR of 4.42 as shown in Fig. 6. The

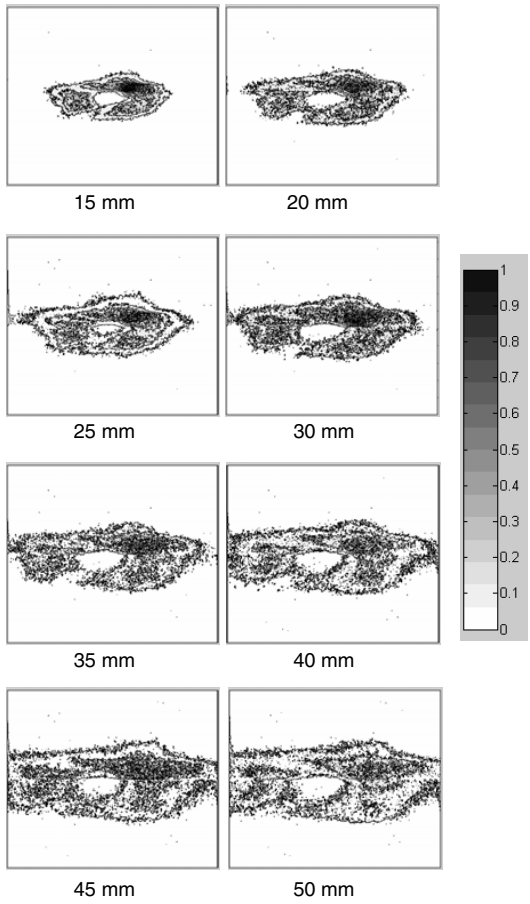

Fig. 5 Volume fraction contour plot in different cross-sectional planes for an ALR of 5.43.

mixing of the liquid in the continuous phase is further delayed when the mass flow rate of the liquid is increased, which is observed from the images. Note that the ALR ratio is decreasing even though the air mass flow is increased. This shows that the internal shear force of the air flow may not be enough to spread the liquid injected into a more uniform sheet when the exit is at atmospheric conditions. Results for other ALRs are presented in [14].

The spray from a prefilming airblast atomizer in a swirl flowfield is generally associated with an asymmetric behavior. In the case of strong swirling flows, the center of the swirl keeps precessing about the axis of symmetry, which is referred to as the precessing vortex core (PVC) [5]. The droplets entrained in the PVC of the strong swirl flow can be observed from the instantaneous PLIF images of flowfields obtained from the patternation measurements. The instantaneous images in Fig. 7 are bisected along the center by doted white lines, and the center of the hollow cone spray from the prefilming airblast atomizer in strong swirl flowfield is marked by a white *X*.

C. Studies on Planar Spray Velocity Field

The axial velocity contour plot of the swirler air velocity field in the absence of the spray is shown in Fig. 8 for an ALR of 7. The central toroidal recirculation zone, which is a characteristic of a high swirl flowfield, can clearly be seen in this figure.

Figure 9 shows the axial velocity contour plot of the spray velocity field for an ALR of 7. The recirculation of the droplets in the flowfield can be seen from this figure. The recirculation region elongates as the air flow through atomizer increases. The maximum velocity of the droplets increases with increase in air mass flow through the atomizer. Significant asymmetry in the velocity distribution of the droplets is attributed to the presence of six guide vanes inside the atomizer liquid passage to impart a tangential component for the

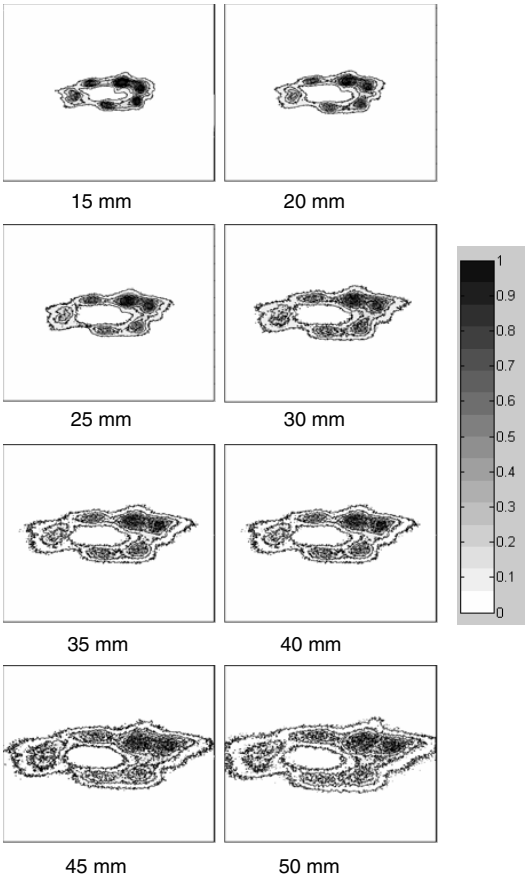

Fig. 6 Volume fraction contour plot in different cross-sectional planes for an ALR of 4.42.

liquid, the proximity of the liquid inlet to the injector location and the inherent properties of the swirl flow.

The mean velocity distributions of spray in different regions in the axial plane of the atomizer are acquired and assembled together to obtain the full flowfield distribution of the droplet velocities from the nozzle in a strong swirl flowfield. The droplets are concentrated between 20 and 30 mm radius at a distance of 10 mm downstream from the atomizer exit. The magnitude of the velocities at this downstream region is less compared with the maximum velocities of the droplets. Figure 10 shows the ensemble-averaged spray velocity vector field for various ALR conditions. The mean velocity of the spray increases with an increase in pressure drop across the atomizer. The stand alone characteristics of the swirler obtained from the PIV studies reveal that the swirl flow is fully developed only beyond 25 mm from the exit plane of the swirler. The droplets come in contact and interact with the air flow from the swirler at this region. The droplets from the spray reach their maximum velocity in a region 30–40 mm downstream from the atomizer exit. In this region, the droplets are broken up into fine particles and they mix well with the air flow. The velocities of the droplets decay further downstream as the corresponding air velocities also decay. Recirculation of droplets is observed along the axis of the atomizer.

The instantaneous velocity vector field of the spray flowfield (not acquired at high frame rates, but at random instants) in a highly three-dimensional air flowfield is shown in Fig. 11. The images show that the droplet flowfield is highly unsteady. It is seen that there is considerable recirculation of droplets having low velocities. The velocity field is characterized by the presence of vortices, with droplets entrained in the vortices thereby undergoing circulatory motion.

D. Droplet Size Distribution

The spray is regarded as a spectrum of drop sizes distributed about some arbitrarily defined mean value. Of the many ways of

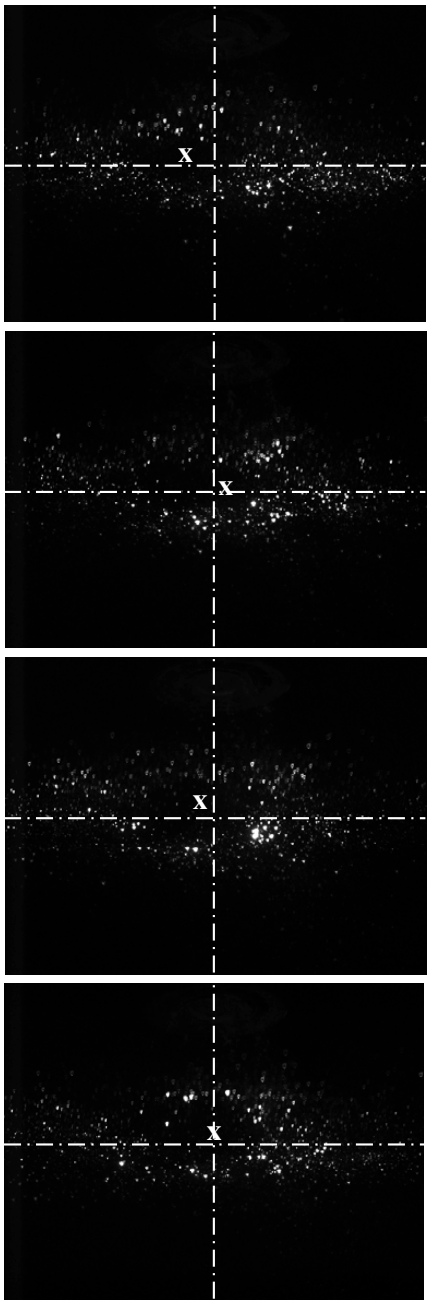

Fig. 7 Instantaneous planar laser-induced fluorescence images.

characterizing sprays, the statistical parameter that is most widely accepted and used is the Sauter mean diameter (SMD). The radial variations of SMD for ALRs of 5.43 and 7.00 at five planes downstream of the atomizer exit are shown in Fig. 12. The maximum SMD coincides with the spray core (note that the spray core is annular, as we are studying a hollow cone spray.) for the planes 12, 20, and 30 mm downstream of the atomizer exit. There is no significant change in the SMD distribution between the regions 12 and 20 mm downstream, except for the expansion in the spray core. The minimum SMD is observed within 5 mm around the axis of the atomizing device axis at all downstream locations. The SMD variation in the radial direction shows local minima for downstream cross-sectional planes 12, 20, and 30 mm from the atomizer exit. The local minima in the SMD are at the periphery of the spray cone. The phenomenon of local minima can be attributed to the action of strong swirling flow on the spray cone. In this region, the swirling air flow imparts a centrifugal force to the droplets in the spray, which carries the bigger droplets toward the outer regions from the atomizer axis; hence, there is an increase in the SMD beyond the local minima. The

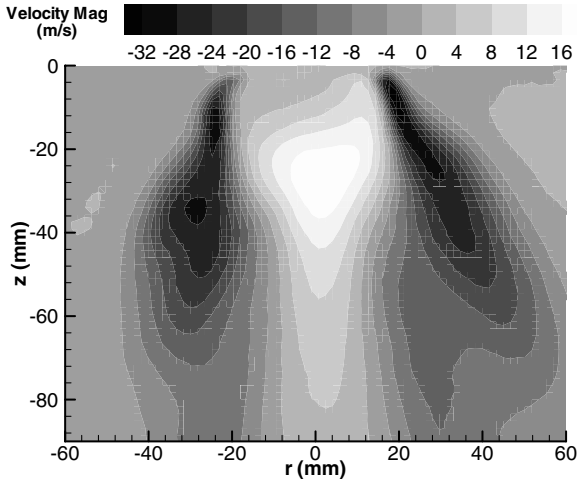

Fig. 8 Ensemble-averaged axial isovelocity contour plot of the air velocity field (in the absence of liquid phase) showing the structure of the CTRZ for test conditions of an ALR of 7.00.

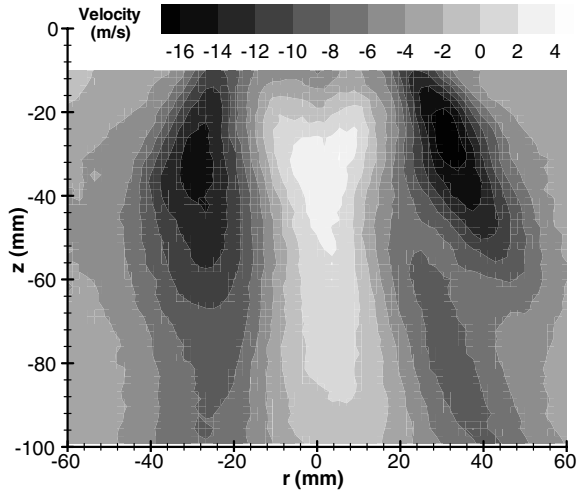

Fig. 9 Ensemble-averaged axial isovelocity contour plot of the droplet velocity of the spray showing the structure of the CTRZ for test conditions of an ALR of 7.00.

trend of local minima is not noticed in cross-sectional planes 40 and 50 mm downstream from the exit of the atomizer; a smoother trend is followed. This is due to the decay of the swirl far downstream and a corresponding decrease in the centrifugal force to bring the large droplets outward.

The SMD of the spray decreases with increase in pressure drop across the atomizer. Finer droplets are detected in the region close to the axis of the atomizer. The droplet size from the atomizer ranges from 0 to 150 μm. The droplet size distribution is in a narrow range of 0–25 μm within a radius of 10 mm from the axis of the atomizer. This reveals that only the smaller size ranges of droplets are entrained in the CTRZ of the strong swirl flow. In between the radii of 20 and 30 mm from the axis of the atomizing device, the maximum number of droplets falls within the size range of 0–60 μm. These radial locations are within the core of the hollow cone spray. Larger droplets are observed at a radial location of 40 mm from the axis of the atomizer. The centrifuging action of the strong swirling flow imparts sufficient radial momentum to the large droplets, which are then carried out radially.

E. Spray Velocity Field

The maximum mean axial velocities of the droplets are in the core of the hollow cone spray from the atomizer, as can be seen from Fig. 13. The maximum magnitude of the mean axial velocities is at

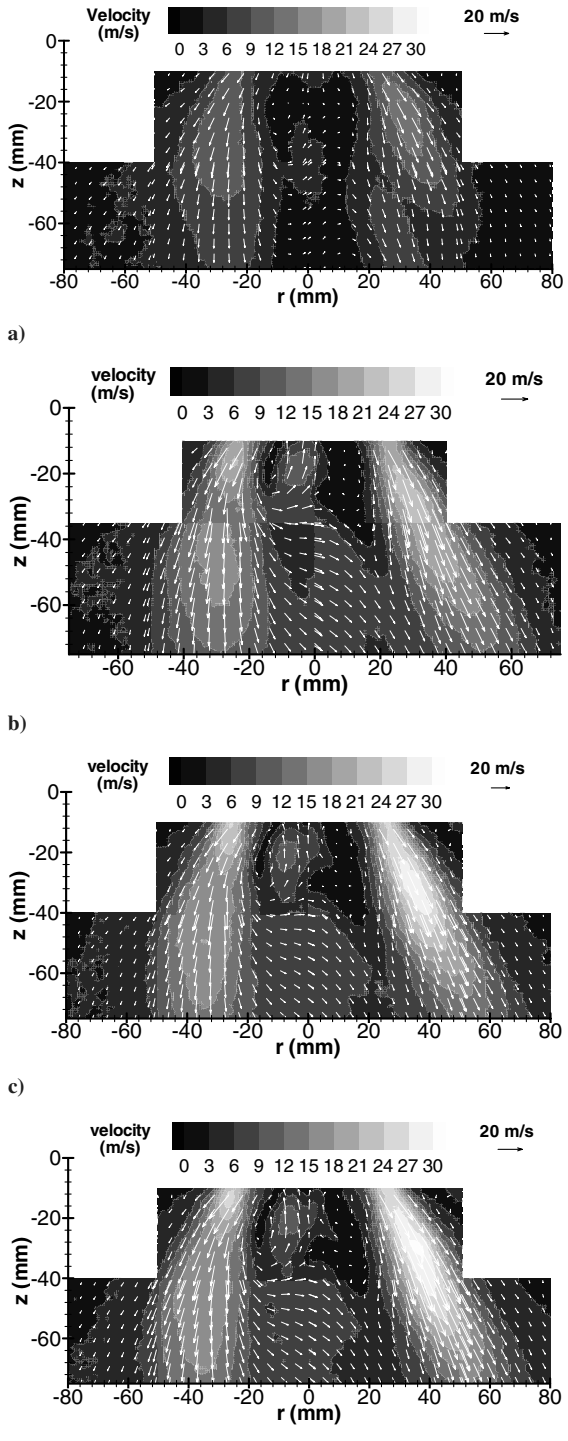

Fig. 10 Ensemble-average droplet velocity vector fields for an a) ALR of 5.43, b) ALR of 7.00, c) ALR of 5.14, and d) ALR of 4.42.

the cross-sectional plane 12 mm downstream from the exit of the atomizer. The mean axial velocities at the cross-sectional plane 12 mm downstream show a narrow region of maximum velocities. The mean axial velocity reaches its maximum between a radius of 20–25 mm from the atomizer axis at the cross-sectional plane 12 mm downstream of the atomizer exit. This region corresponds to the core of the hollow cone spray from the atomizer. The magnitude of the mean axial velocity decreases as we move further downstream from the exit of the atomizer. The reversal in the mean axial velocities of the droplets in the spray is observed along the axis of the atomizer. The region of reversal of mean axial velocities represents the entrainment of droplets in the CTRZ of the strong swirl flow of

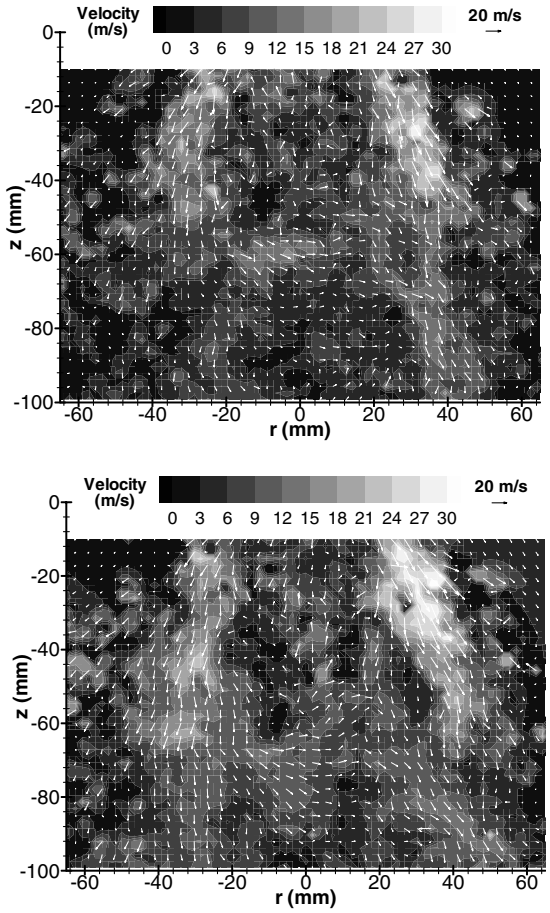

Fig. 11 Instantaneous velocity fields of droplet flowfield for an ALR of 7.00.

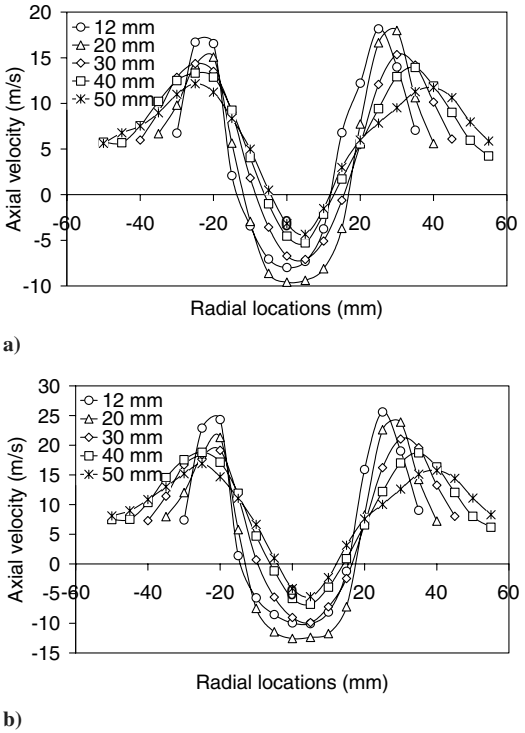

Fig. 13 Radial variation of mean axial velocity of droplets at different planes downstream of the atomizer exit for ALRs of a) 5.43 and b) 7.00.

continuous media from the atomizing device. The magnitude of mean reverse flow velocities of the droplets increases from 12 mm downstream to 20 mm downstream from the exit of atomizing device. The mean axial reverse velocity magnitude of droplets decreases when we move further downstream of atomizer exit from 20 mm.

The mean radial velocity approaches zero at the axis of the atomizing device for the cross-sectional planes 12 and 50 mm downstream of the atomizer exit. Figure 14 shows the mean radial velocity of droplets at different radial locations in cross-sectional

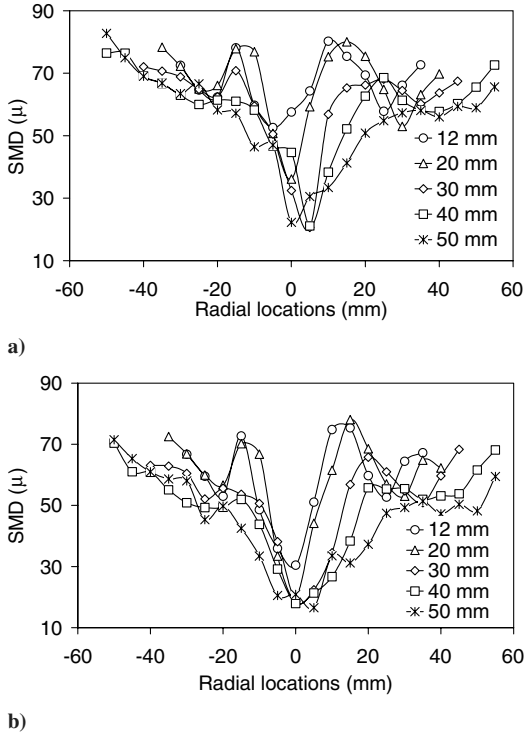

Fig. 12 Radial variation of SMD in a spray field at different planes downstream of the atomizer exit for ALRs of a) 5.43 and b) 7.00.

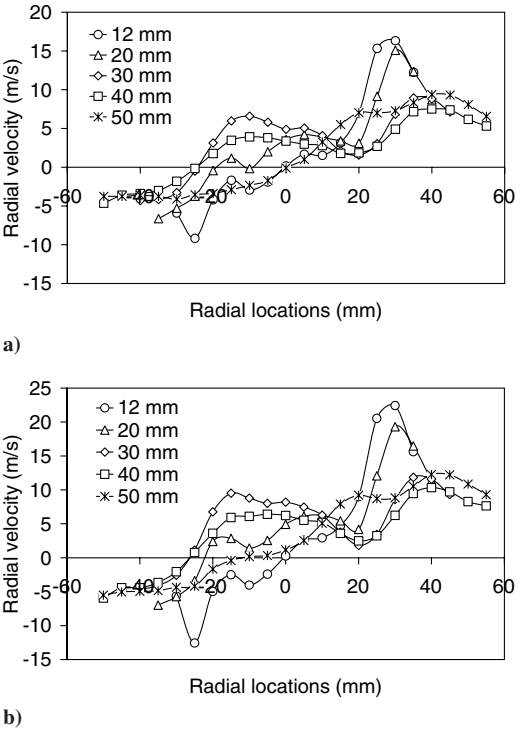

Fig. 14 Radial variation of mean radial velocity of droplets at different planes downstream of the atomizer exit for ALRs of a) 5.43 and b) 7.00.

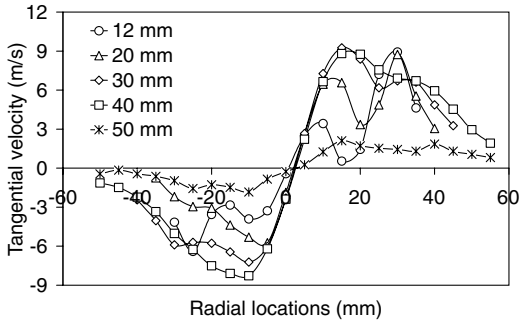

a)

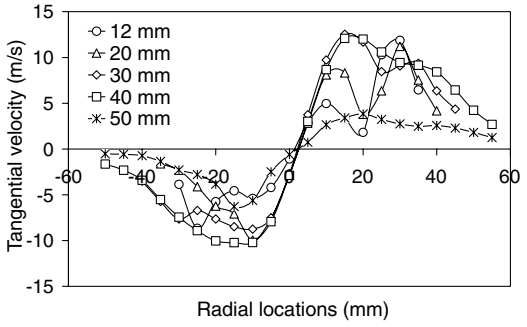

b)

Fig. 15 Radial variation of mean tangential velocity of droplets at different planes downstream of the atomizer exit for ALRs of a) 5.43 and b) 7.00.

planes downstream of the exit of atomizer for AFRs 5.43 and 7.00. The mean radial velocity is way off from zero at the axis of the atomizing device for the downstream cross-sectional planes 20, 30, and 40 mm. The phenomenon of mean radial velocities of droplets not approaching zero at the axis of atomizer is attributed to the entrainment of droplets in the spray in the CTRZ of the strong swirling flow from the atomizing device and asymmetry in the spray, which is evident from the earlier studies [6].

The magnitude of the mean tangential velocity of droplets in the spray alter its direction along the axis of atomizer at all downstream cross-sectional planes from the exit of the atomizer. Figure 15 shows the mean tangential velocity of droplets at different radial locations in cross-sectional planes downstream of the exit of atomizer for AFRs 5.43 and 7.00. The maximum mean tangential velocity of the droplets in the spray is at the cross-sectional planes 30 and 40 mm downstream of the atomizer exit. The mean tangential velocity of droplets increases as we move further downstream up to 30 mm from the exit of the atomizer. There is no considerable change in the mean tangential velocity of the droplets between the cross-sectional planes 30 and 40 mm in most of the radial locations. The mean tangential velocity of the droplets dies down beyond 50 mm from the exit of the atomizer.

The temporal measurement of droplet size and its velocity components in the spray field reveals the random arrival of the droplets and the complexity of the aerodynamic flowfield from the swirler in the atomizer. Figure 16 shows that droplets of various sizes arrive at the probe volume at the same point of time with varying velocities. This is because of the polydisperse nature of the spray from the atomizer. At some locations near the boundary of the CTRZ, the minimum velocities are of the order -10 m/s and the maximum velocities are of the order 25 m/s. At the same location, we can notice the presence of reverse and forward axial velocities for the droplets of smaller size ranges. The presence of the PVC can contribute to the forward and reverse axial velocity at the boundary of the CTRZ. The droplets of bigger size range has more inertia and momentum compared with the smaller size range. Hence bigger size range is not considerably affected by the reverse flow velocities. This behavior of the spray in the recirculation zone helps during combustion to bring the radicals in the combusted products in contact with the unburned mixture.

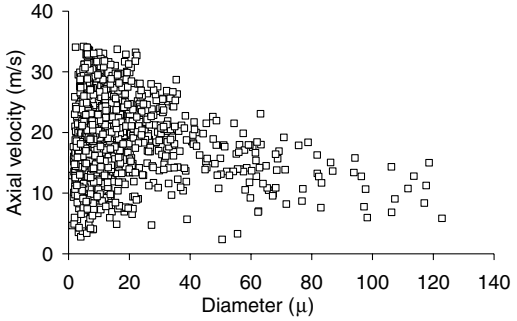

Fig. 16 Individual droplet axial velocities at 20 mm radial location and cross-sectional plane of 30 mm downstream from the exit of the atomizer.

IV. Conclusions

An extensive experimental study for characterizing a highly complex spray flowfield from a prefilming airblast atomizer in a strong swirl flow was performed. Planar Mie Scattering, planar laser-induced fluorescence, two-component particle image velocimetry, and phase Doppler particle-size analyzer/three-component laser Doppler velocimetry were used for characterizing the spray flowfield under atmospheric conditions. Cone angle measurements using flow visualization by planar Mie scattering performed for different air–liquid ratios showed that the spray cone angle increases with increase in the air pressure drop across the atomizer. Instantaneous planar Mie scattering images revealed a high level of unsteadiness in the liquid sheet breakup from the atomizing lip and clusters of droplets in the flowfield. PLIF measurements were used for the patternation of the spray field at several cross-sectional locations. The dispersion of the liquid in the continuous medium is delayed with the increase in the liquid mass flow rate. The planar spray velocity field measurements showed the entrainment of the droplets in the central toroidal recirculation zone of the swirler. Instantaneous velocity vectors of the spray field showed the entrainment of droplets in the vortical structures. The droplet velocities increase with increase in the air mass flow rate. The CTRZ is elongated with increase in air mass flow rate.

The droplet size and the three-component velocities were acquired using a three-component laser Doppler velocimeter and phase Doppler particle-size analyzer. The measurements showed that only small droplets having an SMD less than 25 μm size are present at the CTRZ region. Significant variation in SMD was observed between the cross-sectional planes 30 and 40 mm from the atomizer exit. The phenomena of local minima in SMD was noticed at 12, 20, and 30 mm cross-sectional planes from the atomizer exit. This is because droplets of bigger size ranges are carried radially outward by the centrifugal action of the swirling air flowfield from the atomizer. The SMD decreases with increase in the air mass flow rate. The mean velocity of the droplets increases with increase in pressure drop across the atomizer. The temporal analysis of the measurements showed the high complexity of the spray field in the presence of swirling flow. The velocity measurements show that the strong swirl flow from the atomizing device has its maximum vigor only beyond 30 mm downstream from the exit.

The authors realize the shortcoming of the present investigation, such as atomization at low pressures and the use of water as the liquid. The characteristics of a hollow spray from the prefilming airblast atomizer in strong swirl flowfield is investigated which is a fundamental fluid mechanics problem. Under more realistic engine conditions and while using real fuels, the atomization and, therefore, the spray characteristics, will change. These aspects will have to be covered in subsequent studies.

Acknowledgments

The authors wish to acknowledge the financial support of the Gas Turbine Research Establishment, Bangalore, India and the Extramural Research and Intellectual Property Rights Directorate

of the Defense Research and Development Organization. The interest taken by Venkataraman Shankar, Sampath Kumaran, P. Ramanujam, and G. N. Jayaprakash from the Gas Turbine Research Establishment and by V. Siddhartha from the Extramural Research and Intellectual Property Rights Directorate of the Defense Research and Development Organization in this work is greatly appreciated. We wish to thank Y. Hardalupas, Imperial College of Science, Technology, and Medicine for his advice on the planar laser-induced fluorescence experiments.

References

[1] Han, Y. M., Seol, W. S., Lee, D. S., Yagodkin, V. I., and Jeungm, I. S., "Effects of Fuel Nozzle Displacement on Pre-Fliming Airblast Atomization," *Journal of Engineering for Gas Turbines and Power: Transactions of the ASME*, Vol. 123, No. 1, 2001, pp. 33–40. doi:10.1115/1.1335480

[2] Lefebvre, A. H., and Miller, D., "The Development of an Air Blast Atomizer for Gas Turbine Application," College of Aeronautics Rept. Aero-193, 1996.

[3] Rizkalla, A., and Lefebvre, A. H., "The Influence of Air and Liquid Properties on Airblast Atomization," *Journal of Engineering for Gas Turbines and Power: Transactions of the ASME*, Vol. 97, No. 3, Sept. 1975, pp. 316–320.

[4] Rizk, N. K., and Lefebvre, A. H., "Influence of Liquid Film Thickness on Airblast Atomization," *Journal of Engineering for Gas Turbines and Power: Transactions of the ASME*, Vol. 102, July 1980, pp. 706–710.

[5] Gupta, A. K., Lilley, D. G., and Syred, N., *Swirl Flows*, Energy and Engineering Science Series, Abacus Press, Cambridge, MA, 1984.

[6] Brena de la Rosa, A., Wang, G., and Bachalo, W. D., "The Effect of Swirl on the Velocity and Turbulence Fields of a Liquid Spray," *Journal of Engineering for Gas Turbines and Power: Transactions of the ASME*, Vol. 114, No. 1, Jan. 1992, pp. 72–81. doi:10.1115/1.2906309

[7] Reddy, A. P., Sujith, R. I., and Chakravarthy, S. R., "Swirler Flowfield Characteristics in a Sudden Expansion Square Chamber," *Journal of Propulsion and Power*, Vol. 22, No. 4, 2006, pp. 800–808. doi:10.2514/1.15940

[8] Bazile, R., and Stepowski, D., "2D Laser Diagnostics of Liquid Methanol for Investigation of Atomization and Vaporization Dynamics in a Burning Spray Jet," *25th Symposium (International) on Combustion*, Vol. 25, Combustion Inst., Pittsburgh, PA, 1994, pp. 363–370.

[9] Kelman, B., Sherwood, G., O'Young, F., and Berckmueller, M., "Pulsed Laser Imaging in Practical Combustion systems from 2D to 4D," Optical Diagnostics for Industrial Applications, *Proceedings of SPIE: The International Society for Optical Engineering*, Vol. 4076, No. 55, 2000, pp. 55–65. doi:10.1117/12.397963

[10] Domann, R., and Hardalupas, Y., "A Study of Parameters that Influence the Accuracy of the Planar Droplet Sizing (PDS) Technique," *Particle and Particle Systems Characterization*, Vol. 18, No. 1, 2001, pp. 3–11. doi:10.1002/1521-4117(200102)18:1<3::AID-PPSC3>3.0.CO;2-#

[11] PivView 2C, User Manual, Ver. 2.1, PIVTec GMBH, Germany.

[12] Raffel, M., Willert, C. E., and Kompenhans, J., *Particle Image Velocimetry, A Practical Guide*, Springer–Verlag, New York, 1998, Chaps. 2, 3, 5.

[13] Horender, S., "Experiments and Simulations of Particle-Laden Turbulent Shear Flows," Ph.D. Thesis, Imperial College of Science, Technology and Medicine, London, UK, 2002.

[14] Kumara Gurubaran, R., "Experimental Studies on Prefilming Airblast Atomizer Characteristics," M. S. Thesis, Indian Institute of Technology, Madras, 2005.

[15] Iyer, V. A., and Woodmansee, M. A., "Uncertainty Analysis of Laser-Doppler-Velocimetry Measurements in a Swirling Flowfield," *AIAA Journal*, Vol. 43, No. 3, 2005, pp. 512–519. doi:10.2514/1.8283

D. Talley
Associate Editor